

## Prediction of stress-strain behavior of ceramic matrix composites using unit cell model

Takuya Suzuki<sup>1,a</sup>, Yasuhiro Ohtake<sup>1</sup>, Yoshihiro Otani<sup>1</sup>, Kazuo Yonekura<sup>1</sup> and Yusuke Ueda<sup>2</sup>

<sup>1</sup> Structural Strength Department, Research Laboratory, IHI Corporation, 1, Shin-nakahara-cho, Isogo-ku, Yokohama 235-8501, Japan

<sup>2</sup> Engine Technology Department, IHI Corporation, 3975-18, Haijima-cho, Akishima 196-8686, Japan

**Abstract.** In this study, the elastic modulus and the stress-strain curve of ceramic matrix composites (CMCs) were predicted by using the unit cell model that consists of fiber bundles and matrix. The unit cell model was developed based on the observation of cross sections of CMCs. The elastic modulus of CMCs was calculated from the results of finite element analysis using the developed model. The non-linear behavior of stress-strain curve of CMCs was also predicted by taking the degradation of the elastic modulus into consideration, where the degradation was related to the experimentally measured crack density in CMCs. The approach using the unit cell model was applied to two kinds of CMCs, and good agreement was obtained between the experimental and the calculated results.

### 1. Introduction

Ceramic matrix composites (CMCs) have been expected as a key material for the high performance aerospace engines. The notable advantages of CMCs are high strength and damage tolerance at elevated temperature, which results in improving the efficiency of aerospace engines. To clarify the mechanical performance and the fracture mechanism, many studies have been investigated including the experimental and numerical works [1–8]. For example, A.G. Evans and F.W. Zok [1] provided the review of the physics and mechanics of CMCs. F.W. Zok [2] summarized the discussion in the fracture analysis of CMCs. The industries are also interested in CMCs from the view point of the design and the industrial application. H. Ohnabe et al. [9] and H. Kaya [10] introduced the application of CMCs to the aerospace engine and the automotive ceramic gas turbine. H. Ohya et al. [11] also discussed the structural design of the aerospace engine using CMCs. In general, the structural design requires the elastic modulus and the stress-strain behaviour, where those mechanical properties highly depend on the internal structure of CMCs such as the fiber volume fraction as well as the woven structure. This leads designers to repeat the experiment to obtain the mechanical properties since it is inevitable to modify

---

<sup>a</sup> Corresponding author: [takuya\\_suzuki@ihi.co.jp](mailto:takuya_suzuki@ihi.co.jp)

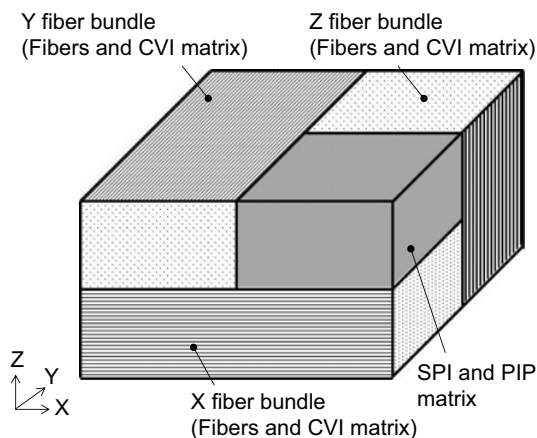


**Figure 1.** Developed unit cell model for the CMC.

the internal structure of CMCs during the design iteration. Consequently, the design of CMCs requires high cost and long time to determine the mechanical properties.

To solve the current problem in designing CMCs, this paper proposes the method to predict the mechanical properties of CMCs from finite element (FE) analysis. The analysis model that is called unit cell model was developed for the simulation. The elastic moduli in several directions and the non-linear behaviour of stress-strain curve of CMCs were predicted by introducing the concept of the damage parameter. The parameter was calculated from the experimentally measured crack densities after the tensile tests of some stress levels. The proposed method was verified using the experimental results of two kinds of CMCs with the different fiber volume fraction. As a result, it was found that the predicted elastic moduli and stress-strain curves of CMCs were in agreement with those of the experimental results even if the fiber volume fraction was different.

## 2. Procedure for predicting mechanical properties of CMCs

### 2.1 Development of unit cell model

The CMC used in this study was constructed with 3-D orthogonal fabric using Tyranno fibers. The fibers were produced at Ube Industries Ltd., and they were woven into the fabric at Shikibo Ltd. The matrix was produced by the combination of chemical vapor infiltration (CVI) process, solid phase infiltration (SPI) process, and polymer impregnation and pyrolysis (PIP) process. The matrix by CVI process was produced around fibers, and the other space was filled with the matrix by SPI and PIP processes. Figure 1 shows the schematic of the unit cell model, where the fiber bundles consist of fibers and CVI matrix, and the matrix consists of those produced by SPI and PIP.

The unit cell model has X, Y and Z fiber bundles. The fiber directions are oriented along X, Y and Z axes in global coordinate system. For fiber bundles, material properties were unknown except for the elastic modulus of the fiber. Therefore, those unknown values were determined from experiments and simulations. For example, considering the fact that the experimentally obtained elastic modulus in Z direction was very low, each fiber bundle was disconnected from others in the simulation. We defined this unit cell model as “non-binding model”, where loads are not transferred between fiber bundles. Although this model is not the real situation, the model gave better prediction for the elastic modulus. The elastic modulus of the matrix in the model was degraded based on the void content since the presence of void was not negligible.

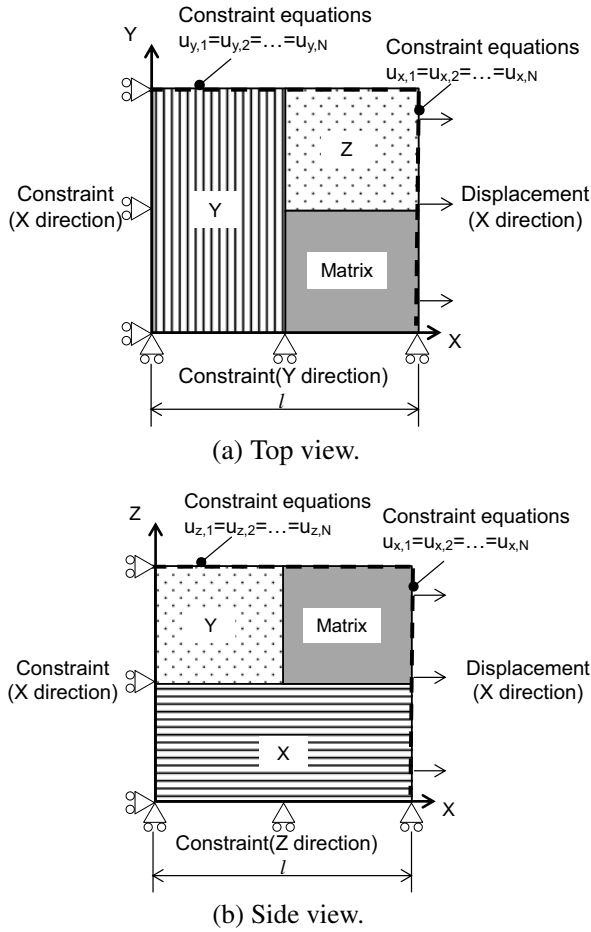


Figure 2. Constraint conditions for FE analysis.

## 2.2 Procedure for calculating elastic modulus of CMCs

The elastic modulus was calculated by numerical tensile test using FE analysis. Figure 2 shows the constraint conditions of the unit cell model when the tensile loading is applied in X direction. The displacement in X direction on the Y-Z surface was constrained, while the displacement was applied on the opposite surface. The displacement in Y direction on the X-Z surface was also constrained, and the constraint equations were defined on the opposite surface, where the displacement of all nodes on the surface was identical. The constraint condition of Z direction was defined by the same way with Y direction. By using the results of FE analysis, homogenized stress  $\Sigma^H$  and homogenized strain  $E^H$  are given by

$$\Sigma^H = \frac{F}{A} \quad (1)$$

$$E^H = \frac{u}{l} \quad (2)$$

where  $F$  is the reaction force on the Y-Z surface,  $A$  is the cross section area of the Y-Z surface,  $u$  is the displacement and  $l$  is the length of the unit cell model in X direction. The elastic modulus  $C^H$  of the

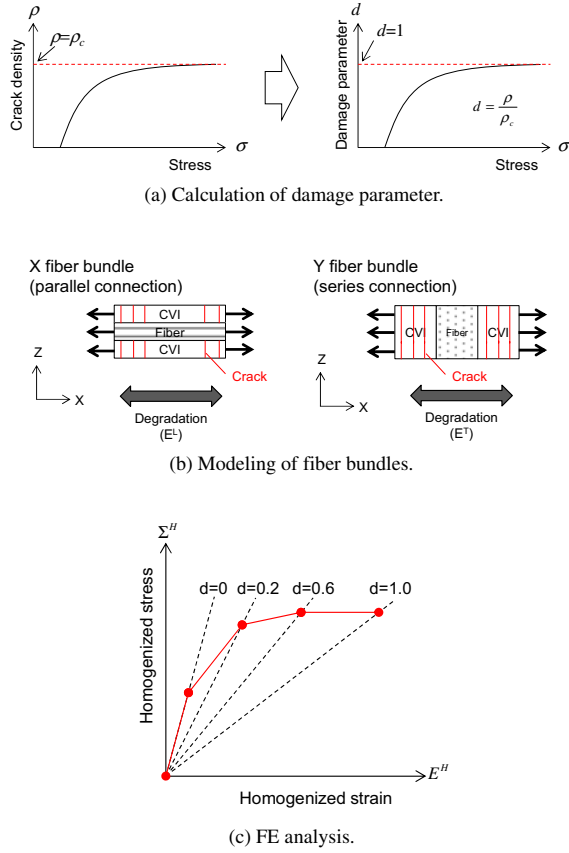


**Figure 3.** Procedure for predicting stress-strain curve.

unit cell model is then calculated as

$$C^H = \frac{\Sigma^H}{E^H} \quad (3)$$

The elastic moduli in other directions are similarly calculated by changing the surface that is subjected to constraint and displacement.

### 2.3 Procedure for predicting stress-strain curve of CMCs

A simulation procedure is proposed to predict the stress-strain curve of the CMC by taking the degradation of the elastic modulus into consideration. Figure 3 shows the procedure for predicting stress-strain curve. To simplify the explanation, we considered the case in which the load is applied in X direction. The details of the procedure are provided in the following steps.

First, the tensile tests are performed for several kinds of loads before the specimens are fractured. After the tensile tests, the length of each crack is measured by observing the cross sections of the specimens using microscope and the crack densities are calculated. The definition of the crack density is

$$\rho = \frac{1}{S} \sum_i \lambda_i \quad (4)$$

where  $\rho$  is the crack density,  $S$  is the observed cross section area and  $\lambda_i$  is the length of  $i$ -th crack. As a result, the relationship between stress and the crack density is obtained as shown in Fig. 3(a).

Second, the elastic modulus of fiber bundles is degraded with increasing the crack density since the cracks were observed in CVI matrix and they grew during the tensile tests. We introduce damage parameter  $d$  to define degradation of the elastic modulus. The damage parameter is defined as

$$d = \frac{\rho}{\rho_c} \quad (5)$$

where  $d$  is the damage parameter and  $\rho_c$  is a critical crack density. We regarded  $\rho_c$  as saturated crack density as shown in Fig. 3(a). The orthotropic cracking behavior is also taken into consideration as shown in Fig. 3(b). Figure 3(b) denotes that the elastic modulus of X fiber bundles is degraded only in fiber direction and that of Y fiber bundles is degraded only in transverse direction. By using damage parameter  $d$  in Eq. (5), the degradation of the elastic modulus of the CVI matrix is given by

$$E'_{CVI} = (1 - d)E_{CVI} \quad (6)$$

where  $E_{CVI}$  is the initial modulus of CVI matrix and  $E'_{CVI}$  is the degraded one. The elastic modulus of fiber bundles is then calculated as a combination of fibers and CVI matrix. The effective modulus in fiber direction is calculated as a parallel connection of fibers and matrix, and that in transverse direction is calculated as a series connection of them. By considering the cracks in CVI matrix, the elastic moduli are then given by

$$E_X^L = \frac{V_f E_f^L + V_{CVI} E'_{CVI}}{V_f + V_{CVI}} = \frac{V_f E_f^L + V_{CVI} (1 - d_x) E_{CVI}}{V_f + V_{CVI}} \quad (7)$$

$$E_X^T = \frac{(V_f + V_{CVI}) E_f^T E_{CVI}}{V_f E_{CVI} + V_{CVI} E_f^T} \quad (8)$$

$$E_Y^L = \frac{V_f E_f^L + V_{CVI} E_{CVI}}{V_f + V_{CVI}} \quad (9)$$

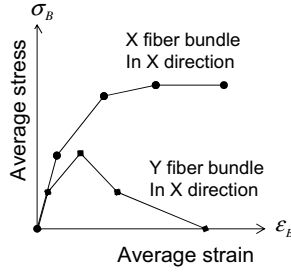
$$E_Y^T = \frac{(V_f + V_{CVI}) E_f^T E'_{CVI}}{V_f E'_{CVI} + V_{CVI} E_f^T} = \frac{(V_f + V_{CVI}) E_f^T (1 - d_y) E_{CVI}}{V_f (1 - d_y) E_{CVI} + V_{CVI} E_f^T} \quad (10)$$

where  $E_X^L$  and  $E_X^T$  are the elastic modulus of fiber direction and transverse direction for X fiber bundles,  $E_Y^L$  and  $E_Y^T$  are those of Y fiber bundles,  $E_f^L$  and  $E_f^T$  are those of fibers, and  $V_f$  and  $V_{CVI}$  are volume fraction of fiber and CVI matrix.

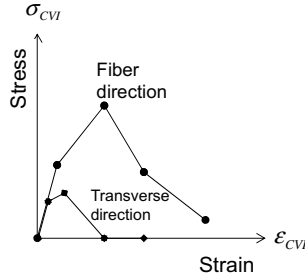
Finally, FE analysis is performed for each stress level by using correspondingly degraded elastic modulus of fiber bundles. Here, the linear orthotropic material is defined for each fiber bundles using from Eq. (7) to Eq. (10). The homogenized stress and strain are calculated by Eqs. (1) and (2). As shown in Fig. 3(c), the stress-strain curve of the CMC is derived after several times of calculation.

The above mentioned procedure is only available when the crack density is obtained for CMCs of a target. This means that the crack density needs to be measured respectively when the fiber content or the woven structure of CMCs are changed. To predict the stress-strain curve for any kinds of CMCs, we derived a non-linear stress-strain curve of CVI matrix that is independent from the fiber content or the woven structure.

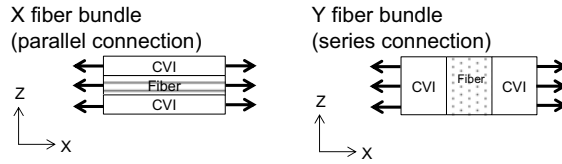
The procedure for predicting the stress-strain curve of any CMCs is shown in Fig. 4. The stress-strain curve of CVI matrix is calculated from the results of linear analysis. The average stress and strain of fiber bundles are calculated at each stress levels as shown in Fig. 4(a). Considering that the fiber bundles are modeled as parallel and series connection of fibers and matrix, the stress and strain of CVI matrix



(a) Average stress and strain of fiber bundles.



(b) Stress-strain curve of CVI matrix.



(c) Modeling of fiber bundles.

**Figure 4.** Procedure for calculating stress-stain curve of CVI matrix and predicting that of any CMCs.

are calculated as

$$\sigma_{CVI}^L = \frac{(V_f + V_{CVI})\sigma_B^L - V_f E_f^L \epsilon_f^L}{V_{CVI}} \quad (11)$$

$$\epsilon_{CVI}^L = \epsilon_B^L \quad (12)$$

$$\sigma_{CVI}^T = \sigma_B^T \quad (13)$$

$$\epsilon_{CVI}^T = \frac{1}{V_{CVI}} \left\{ (V_f + V_{CVI})\epsilon_B^T - V_f \frac{\sigma_f^T}{E_f^T} \right\} \quad (14)$$

where  $L$  is fiber direction,  $T$  is transverse direction and  $B$  is fiber bundle. By connecting these results, the stress-strain curve of CVI matrix is obtained as shown in Fig. 4(b).

The stress-strain curve of any CMCs is then calculated using fiber content of the target CMC, where the fiber bundles of the target CMC is modeled as parallel and series connection of fibers and matrix

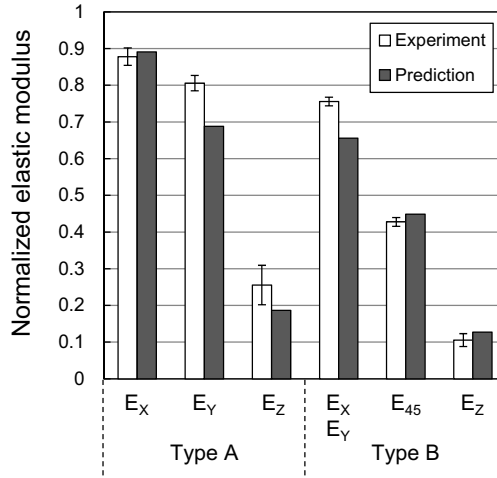


**Figure 5.** Comparison of experimental and calculated elastic moduli.

as shown in Fig. 4(c). Finally, non-linear material model of Fig. 4(c) is used in FE analysis and the stress-strain curve of the target CMC is predicted.

### 3. Numerical results

#### 3.1 Estimation of the elastic modulus of CMCs

The proposed calculation method of the elastic modulus was applied to two kinds of unit cell models; here we define them as type A and type B. A schematic of the unit cell model is shown in Fig. 1. The unit cell models of types A and B have different fiber content in bundles and different amount of fiber bundles in the unit cell. The commercial finite element software ABAQUS ver.6.11 was used. Figure 5 shows a comparison of predicted elastic moduli and experimental results of types A and B, where  $E_x$ ,  $E_y$ ,  $E_z$  and  $E_{45}$  are the elastic moduli of X, Y, Z and 45 degree respectively. Considering the scatter of experimental data, predicted moduli are in agreement with experimental results.

#### 3.2 Estimation of the stress-strain curve of CMCs

The stress-strain curve was predicted for the CMC of type A using the procedure of Fig. 3. We performed tensile tests and calculated the crack density at each stress level. Figure 6 shows the relationship between the crack density and the applied stress, where each data is normalized with maximum value. Since the crack density of X and Y fiber bundles increased monotonically, we regarded extrapolated crack density as  $\rho_c$  and calculated damage parameters as shown in Fig. 7. The elastic modulus was calculated using from Eq. (6) to Eq. (10) and FE analysis was performed at each stress level to predict the stress-strain curve. Figure 8 shows the experimental and predicted curves for the CMC of type A, where stress and strain are normalized. The overall behavior of the stress-strain curve was predicted well using the proposed procedure.

The prediction of the stress-strain curve for the CMC of type B was also performed. According to the procedure of Fig. 4, the stress-strain curve of CVI matrix was calculated for fiber direction and transverse direction respectively as shown in Fig. 9. Figure 10 denotes the non-linear stress-strain curve of fiber bundles for the CMC of type B. Figure 11 shows a comparison of stress-strain curve obtained

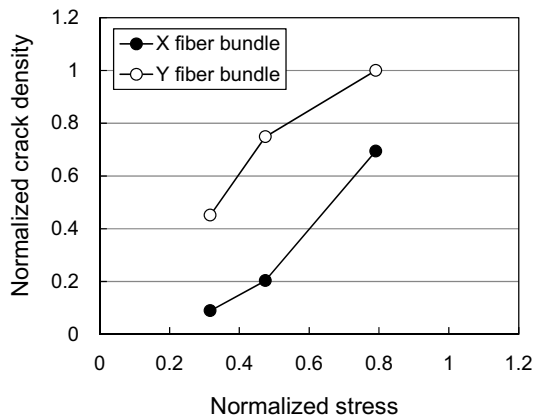


Figure 6. Relationship of normalized crack density and normalized stress for the CMC of type A.

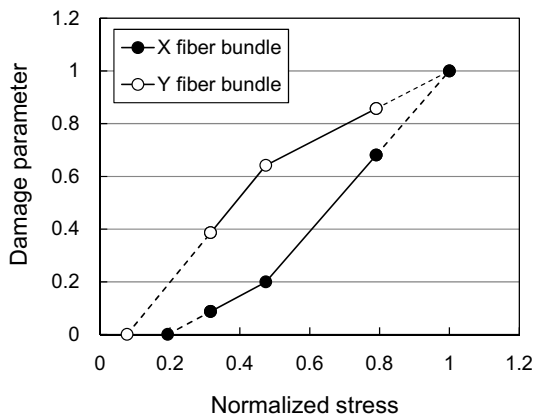


Figure 7. Relationship between damage parameter and normalized stress for the CMC of type A.

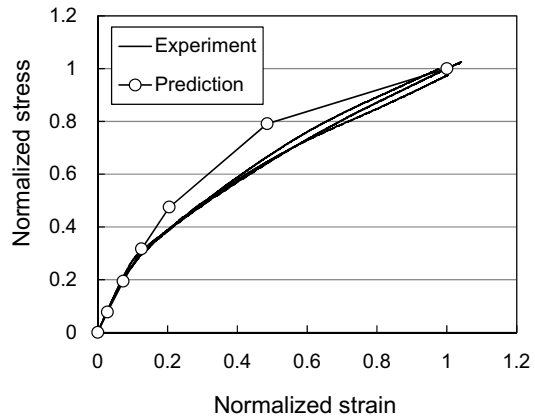


Figure 8. Comparison of experimental and predicted results of stress-strain curve for the CMC of type A.

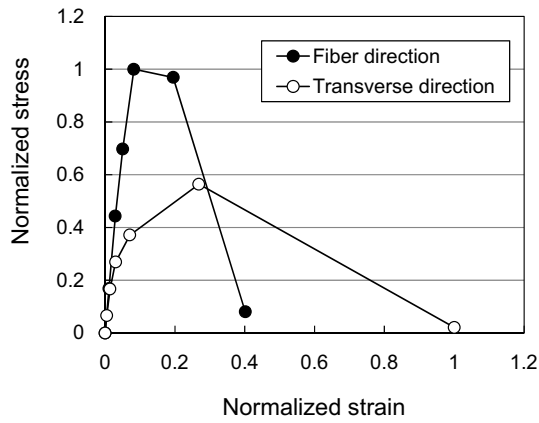


Figure 9. Stress-strain curve of CVI matrix.

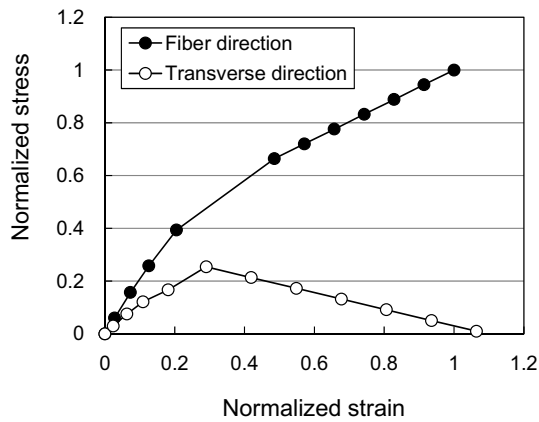


Figure 10. Stress-strain curve of fiber bundles for the CMC of type B.

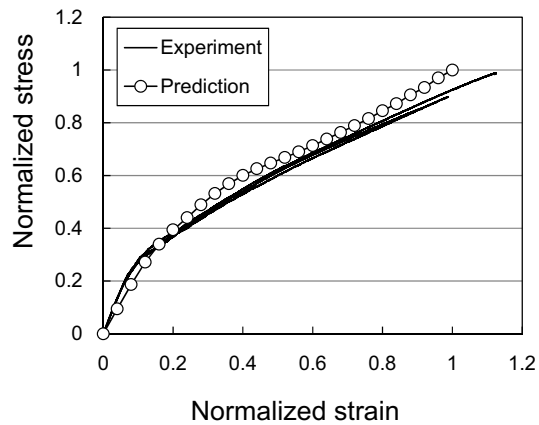


Figure 11. Comparison of experimental and predicted results of stress-strain curve for the CMC of type B.

by experiment and non-linear analysis. Since the non-linear behavior was predicted well, it was verified that the proposed method can be applied to different kinds of CMCs.

#### 4. Conclusions

In this study, the elastic modulus and non-linear stress-strain curve of the CMC were predicted by using unit cell model. The unit cell model of the CMC was made with fiber bundles and matrix, which was determined from the observation of cross sections. For the calculation of the elastic modulus of the CMC, the homogenized stress and strain were introduced. The degradation of elastic modulus of fiber bundles was also taken into consideration for the prediction of stress-strain curve, where the degradation was related to experimentally measured crack density. Furthermore, the method for calculating the stress-strain curve of CVI matrix in the CMC was proposed and non-linear stress-strain curve of any CMCs became to be predicted.

The elastic moduli and the stress-strain curves of two kinds of CMCs were predicted along the proposed method. The elastic moduli of several directions were in agreement with the experimental results. The overall behavior of the stress-strain curve was also predicted well. Therefore, it was verified that the proposed method can be applied to different kinds of CMCs.

However, it is noted that further studies should be performed to improve the accuracy of the prediction. For example, the unit cell model based on the non-binding model should be improved since this is not the real situation. The scatter of the crack density should be considered since the experimental data were not enough in this study.

#### References

- [1] A.G. Evans, F.W. Zok, *J. Mater. Sci.* **29**, 3857 (1994)
- [2] F.W. Zok, *ASM handbook* **21**, 407 (2001)
- [3] W.A. Curtin, *J. Am. Ceram. Soc.* **74**, 2837 (1991)
- [4] H. Cao, M.D. Thouless, *J. Am. Ceram. Soc.* **73**, 2091 (1990)
- [5] J.C. McNulty, F.W. Zok, *J. Am. Ceram. Soc.* **80**, 1535 (1997)
- [6] D. Lue, S. Takezono, K. Tao, H. Minamoto, *Int. J. Damage Mech.* **12**, 141 (2003)
- [7] A. Burr, F. Hild, F.A. Leckie, *Mater. Sci. Eng.* **A250**, 256 (1998)
- [8] J.L. Kuhn, S.I. Haan, P.G. Charalambides, *J. Comp. Mater.* **34**, 1640 (2008)
- [9] H. Ohnabe, S. Masaki, M. Onozuka, K. Miyahara, T. Sasa, *Compos. Part A Appl. Sci. Manuf.* **30**, 489 (1999)
- [10] H. Kaya, *Compos. Sci. Technol.* **59**, 861 (1999)
- [11] H. Ohya, N. Natsumura, Y. Ohtake, K. Takahashi, T. Nakamura, S. Masaki and H. Ohnabe, *Proceedings of the 10<sup>th</sup> International Symposium on Ultra-High Temperature Materials*, 65 (1996)